

Interconverting Hydrogen-Bonding and Weak $n \rightarrow \pi^*$ Interactions in Aqueous Solution: A Direct Spectroscopic Evidence

Pranab Deb,^{‡,§,#} Geun Young Jin,^{||,⊥,#} Santosh K. Singh,[†] Juran Moon,^{||} Hyejin Kwon,^{||} Alope Das,^{*,†} Sayan Bagchi,^{*,‡,§} and Yung Sam Kim^{*,||}

[†]Department of Chemistry, Indian Institute of Science Education and Research (IISER), Dr. Homi Bhabha Road, Pune 411008, India

[‡]Physical and Materials Chemistry Division, CSIR-National Chemical Laboratory (CSIR-NCL), Dr. Homi Bhabha Road, Pune 411008, India

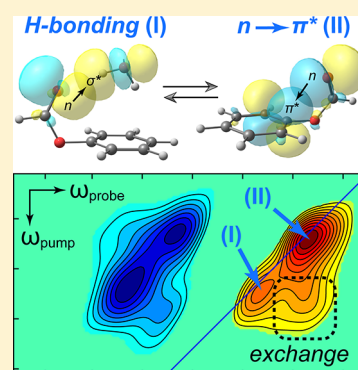
[§]Academy of Scientific & Innovative Research (AcSIR), CSIR-National Chemical Laboratory (CSIR-NCL), Dr. Homi Bhabha Road, Pune 411008, India

^{||}Department of Chemistry, Ulsan National Institute of Science and Technology (UNIST), 50 UNIST-gil, Ulsan 44919, Republic of Korea

[⊥]Department of NanoFusion Technology, Pusan National University, Busan 46241, Republic of Korea

Supporting Information

ABSTRACT: Molecular structure and function depend on myriad noncovalent interactions. However, the weak and transient nature of noncovalent interactions in solution makes them challenging to study. Information on weak interactions is typically derived from theory and indirect structural data. Solvent fluctuations, not revealed by structure analysis, further complicate the study of these interactions. Using 2D infrared spectroscopy, we show that the strong hydrogen bond and the weak $n \rightarrow \pi^*$ interaction coexist and interconvert in aqueous solution. We found that the kinetics of these interconverting interactions becomes faster with increasing water content. This experimental observation provides a new perspective on the existence of weak noncovalent interactions in aqueous solution.



The delicate balance between the formation and disruption of different noncovalent interactions orchestrates molecular structure, stability, and function in solution.^{1,2} The hydrogen bond (H bond), prevalent in chemistry and biochemistry, is a well-studied noncovalent interaction. The importance of weaker H bonds has grown in recent times.^{3–6} Weaker H-bond interactions such as C–H···A (A = N, O, or S), D–H··· π (D = N or O), and C–H··· π have been shown to exist in nature.⁷ Analogous to the H-bond interactions, where lone-pair electrons are delocalized into a σ^* orbital of an acceptor moiety ($n \rightarrow \sigma^*$),⁸ the carbonyl (C=O) group can participate in weak noncovalent interactions with the acceptor's π^* orbital ($n \rightarrow \pi^*$). $n \rightarrow \pi^*$ interactions involving electron delocalization from an oxygen lone pair to the antibonding π^* orbital of either another carbonyl ($n \rightarrow \pi^*_{\text{C=O}}$) or an aromatic ring ($n \rightarrow \pi^*_{\text{ar}}$) have strong presence in nucleic acids,^{9–11} proteins,^{12,13} supramolecular assemblies,^{14,15} and small molecules.^{16–20}

Although analogous in terms of electron delocalization, a large disparity exists between the interaction energies of the C=O H bond and the $n \rightarrow \pi^*$ interaction. Calculations have estimated a typical $n \rightarrow \pi^*$ interaction to be energetically weaker (0.3–1.5 kcal/mol) than the H bond (4–10 kcal/

mol).¹² Thus, even though $n \rightarrow \pi^*$ interactions have been found in the crystal structures, the origin of the coexistence of this weak interaction with a stronger competitor like an H bond is unknown. Moreover, the interplay between a weak $n \rightarrow \pi^*$ interaction and a strong H bond in solution is further complicated by solvent dynamics and conformational fluctuations.

Because both the interactions involve oxygen lone-pair electrons, any interplay between them is likely to affect the key aspects of chemistry and chemical biology. Despite the importance, the reason behind our dearth of knowledge about $n \rightarrow \pi^*$ interactions in solution is two-fold. First, other than a recent gas-phase spectroscopic study on phenyl formate (PF),²¹ the information on weak $n \rightarrow \pi^*$ interactions has been derived indirectly, from either X-ray crystal structure analyses (Protein Data Bank and Cambridge Structural Database) or ab initio calculations.^{10,22,23} Installing isosteric substituents, Raines and coworkers reported $n \rightarrow \pi^*$ interactions in small-

Received: August 5, 2018

Accepted: August 27, 2018

Published: August 27, 2018

molecule esters and amides by combining structural data from X-ray diffraction, NMR spectroscopy, and ab initio calculations.^{12,24,25} Second, the direct IR spectroscopic evidence of the $n \rightarrow \pi^*$ interaction in PF was obtained in an isolated environment (gas phase) in the absence of any competing H bond. A spectroscopic approach that includes information on solvent and conformational dynamics is necessary to probe the relative importance of H-bonding and $n \rightarrow \pi^*$ interactions. Two-dimensional infrared (2D IR) spectroscopy^{26–34} monitors the time evolution of energetically distinct C=O populations in solution with femtosecond time resolution and allows quantitative investigation of the role of solvent fluctuations on the noncovalent interactions involving the C=O moiety.

Das and coworkers monitored the C=O stretch of PF using isolated gas-phase IR spectroscopy and reported two populations arising from cis and trans conformers.²¹ In the cis conformer, the lone-pair electrons on the C=O oxygen are delocalized into the π^* orbital of the phenyl ring. In the gas phase, the cis conformer participating in $n \rightarrow \pi^*$ interactions is more stable than the trans conformer, where the C=O rotates away from the ring. Herein, using linear IR and 2D IR spectroscopy in aqueous solution, we report the first observation and measurement of solvent-mediated coexistence and interconversion between the energetically disparate $n \rightarrow \pi^*$ interaction and H bonding. In addition, we have used density functional theory (DFT), molecular dynamics (MD) simulations, and natural bond orbital (NBO) analysis³⁵ to interpret the spectral changes and confirm the presence of $n \rightarrow \pi^*$ interactions in solution.

To obtain a comparison with the gas-phase results,²¹ a solution-phase IR spectrum of PF was obtained in a nonpolar aprotic solvent, tetrahydrofuran (THF, $\epsilon = 7.4$). In accordance with the gas-phase results, the IR spectrum in THF shows two C=O transitions (1766 and 1744 cm^{-1} , Figure 1a). Peak positions in THF are red-shifted from the reported gas-phase peak positions (1797 and 1766 cm^{-1} , Figure 1a).²¹ The lowering of the C=O frequencies is common going from the gas phase to the solution phase.³⁶ IR spectra in other aprotic solvents also show two C=O transitions (Figure S1). Structural assignments for the two PF conformers in THF were obtained from DFT calculations performed at the M05-2X level of theory using polarizable continuum model (PCM, see the Supporting Information for details). DFT-estimated C=O peak frequencies of the two conformers in THF are in consonance with the experimental results (Table S1). The optimized geometries of the conformers in aprotic solvent are similar to those in the gas phase (Table S2 and Figure S2).²¹

To gain a greater insight into the origin of the noncovalent interaction of the cis conformer in THF, we have performed an NBO analysis of the optimized geometry (Figure 1e). The second-order perturbative energy ($E_{n \rightarrow \pi^*}^{(2)}$) in the cis conformer (1.41 kcal/mol) confirms the presence of the $n \rightarrow \pi^*$ interaction. The possibility of an intramolecular CH \cdots O H bonding was eliminated based on NBO predictions and geometrical parameters (Table S3 and Figure S3, Supporting Information).

To investigate the $n \rightarrow \pi^*$ interactions when C=O can competitively form an H bond with solvent, the IR spectrum of PF was obtained in water (D_2O). The IR spectrum in water shows signatures of C=O H bonding as the overall spectrum shifts to lower frequencies (Figure 1c). The spectrum can apparently be fitted to four peaks using Voigt lineshapes,

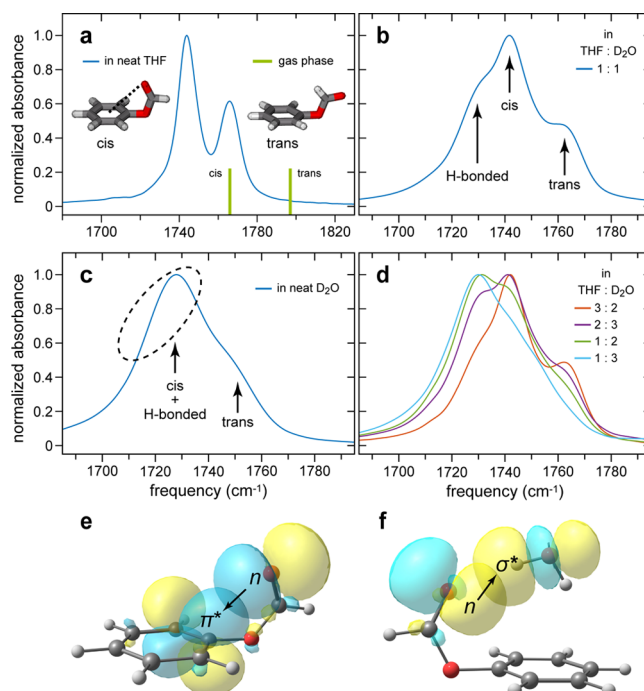


Figure 1. Linear IR spectra of PF in (a) neat THF, (b) 1:1 THF/D₂O (v/v), (c) neat D₂O, and (d) different aqueous THF solutions. The green lines in panel a correspond to the peak positions in the gas phase.²¹ Orbitals corresponding to (e) $n_{\text{CO}} \rightarrow \pi^*_{\text{ar}}$ and (f) $n_{\text{CO}} \rightarrow \sigma^*$ (H-bond) NBO interactions for the cis and the H-bonded conformers.

consisting of two additional C=O peaks at 1704 (11%) and 1724 cm^{-1} (44%) along with the peaks in THF for the trans (11%) and the cis (34%) conformations (Table S4 and Figure S4a, Supporting Information). The additional peak positions agree with the reported ester C=O transitions in water due to one and two C=O H bonds.^{37–39}

To further interrogate the coexistence of the $n \rightarrow \pi^*$ and the H-bonding interactions, we performed IR experiments on PF in aqueous THF solutions by systematically varying the water content from 20 to 80% (v/v) (Figure 1b,d, and Figure S4). Fitting each spectrum with multiple Voigt lineshapes indicates that an increase in water content causes a decrease in the trans and the cis populations along with a concomitant increase in the H-bonded C=O population (Figure 2, Figure S4, and Tables S4–S11). A similar spectral trend is seen in aqueous solutions of other aprotic solvents (Figure S5). At higher water concentrations, evidence of the double-H-bonded population is observed (Tables S4–S11); a similar observation has been previously reported.⁴⁰ IR spectra in aqueous solutions clearly demonstrate the coexistence of a conformer with an internal $n \rightarrow \pi^*$ interaction and a conformer in which C=O H-bonds to solvent. However, information on the role of solvent dynamics is missing.

DFT calculations, performed on PF with a single water molecule, indicate that water preferably interacts with the cis conformer and simultaneously forms an H bond with the C=O and an O–H \cdots π interaction with the arene (Figure S6). A subsequent NBO calculation predicts the H-bond interaction energy to be 4.2 kcal/mol, which is approximately three times the estimated $n \rightarrow \pi^*$ interaction energy in the cis conformer. Atomistic MD simulations, performed on PF in neat water to obtain a better representative picture of the experiments,

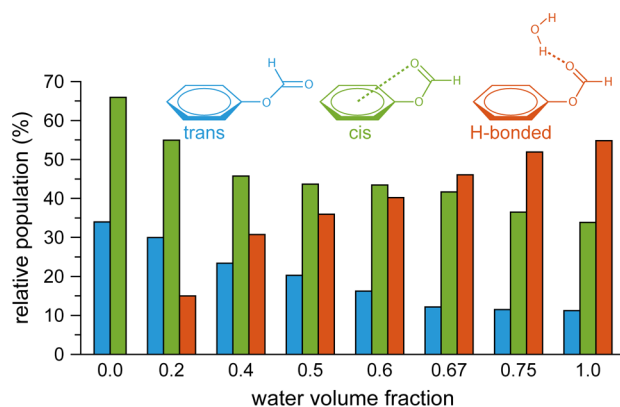


Figure 2. Relative conformational population with varying water content in aqueous THF solutions. The H-bonded population includes both single and double H bonds to C=O.

predict that the PF C=O is predominantly single H-bonded to water ($\sim 56\%$), along with a 12% double H-bonded and a 32% non-H-bonded population. This is in qualitative agreement with our IR absorption results. The single-water DFT calculation has only the enthalpic component and predicts the bridged configuration. MD simulations, with both enthalpy and entropy contributions, show the single H-bonded C=O is most probable in bulk water. MD trajectories, however, predict a non-negligible non-H-bonded population. Simulations also predict the C=O group in the trans conformer to form an H bond, but the broad C=O IR H-bonded peak provides little information on whether the H bonding is cis or trans (see the [Supporting Information](#)).

To capture the effect of solvent and conformational dynamics on the coexistence of the H bond and the $n \rightarrow \pi^*$ interaction, we performed 2D IR spectroscopy. 2D IR utilizes three interactions of ultrashort femtosecond pulses at different time delays to generate a nonlinear signal. Details of 2D IR are given in the [Supporting Information](#) (Figures S7–S9). 2D IR spectra (Figure 3) of PF with multiple C=O populations, plotted at different time delays (T), consist of multiple diagonal peaks from the overlapping conformational distributions in the corresponding linear IR spectrum. Interconversion between conformations gives rise to cross peaks that evolve with T . The T -dependent evolution of the cross peaks is a direct spectroscopic signature of conformational interconversion arising from breaking and reformation of noncovalent interactions during equilibrium dynamics.^{40–46}

We observe T -dependent evolution of cross peaks between the cis conformer and the H-bonded conformer in the 2D IR spectra of PF dissolved in a series of THF/water solutions (Figure 3), a direct evidence supporting a picosecond time-scale interconversion between the conformer with an $n \rightarrow \pi^*$ interaction and a conformer with an H-bonding interaction to solvent. To analyze the interconversion kinetics in each THF/water composition, we performed least-squares fitting of the corresponding numerically simulated 2D IR spectrum (Figures S10–S15).^{40,42} The estimated kinetic rates (Table S12) reveal that the interconversion between the strong and the weak interactions is accelerated with the increase in the water content (Figure 4).

The interconversion time scale is the fastest in neat water (~ 1.5 ps), in agreement with water's H-bond breaking and reformation time scale.⁴² A decrease in water content leads to a gradual slow-down of the exchange rate, with a 13-fold (~ 20

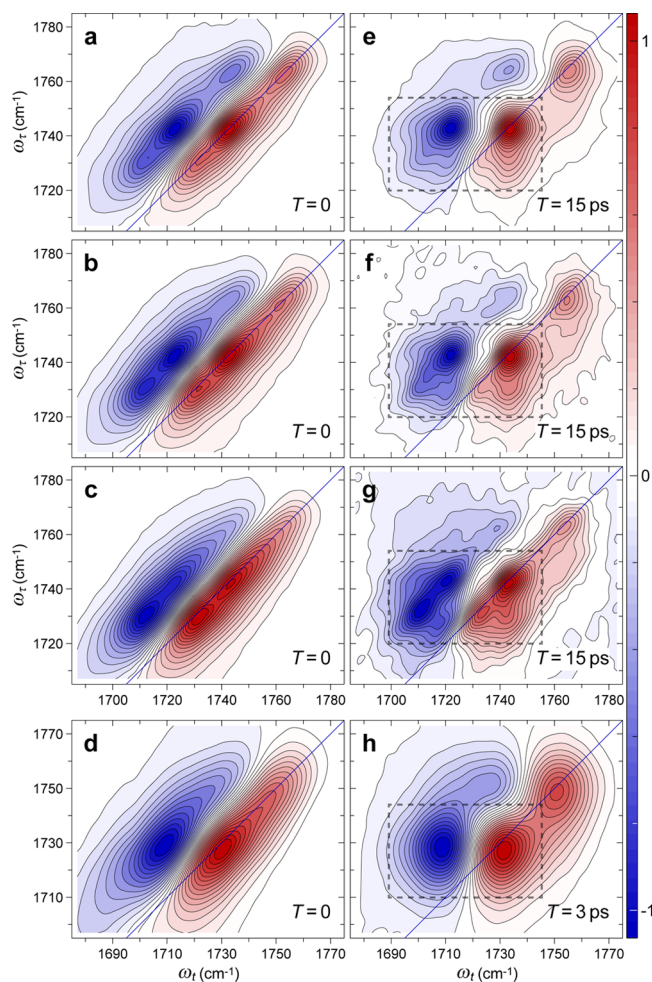


Figure 3. 2D IR spectra with varying water content at different T values. 2D IR spectra of PF at $T = 0$ in (a) 1:1 THF/water, (b) 2:3 THF/water, (c) 1:2 THF/water, and (d) neat water. (e–g) 2D IR spectra at $T = 15$ ps for corresponding THF/water solutions and (h) at $T = 3$ ps in neat water. The diagonal peak pairs show three C=O populations arising from trans, cis ($n \rightarrow \pi^*$), and H-bonded conformers of PF in the order of decreasing frequencies. The cross peaks between the cis and the H-bonded conformations evolve as T increases. The dashed rectangles in panels e–h encompass regions of the cross peaks.

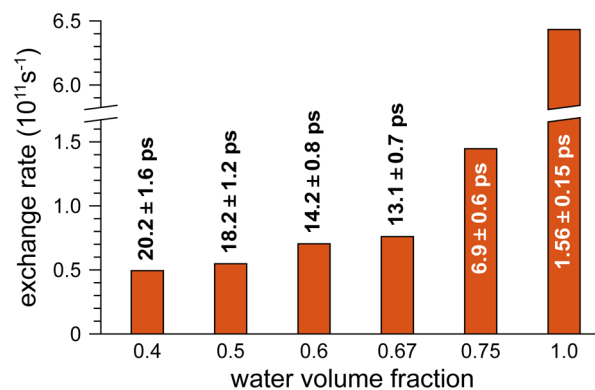


Figure 4. Interconversion rates and the corresponding time scales in different THF/water mixtures.

ps) decrease in 40% water (nonideality of THF/water mixtures plays negligible role in the slowdown; see the [Supporting](#)

Information). No experimental evidence, however, was observed for the H-bond dynamics of the trans conformer. This is probably due to the limitation in the detection limit arising from the smaller population of the non-H-bonded trans conformer population. Furthermore, interconversion between non-H-bonded cis and trans conformers was not found in solutions up to 70% water content within the 2D IR experimental time window. The weak signal from the reduced trans population makes it difficult to comment on cis–trans isomerization at higher water content. Distinct cross peaks are only observed between C=O populations that are either H-bonded or engaging in the $n \rightarrow \pi^*$ interaction.

To date, interpretations regarding the existence of the weak $n \rightarrow \pi^*$ interactions in aqueous solution utilized statistical surveys of static crystal structures²² and NBO calculations.⁴⁷ However, 2D IR results provide direct evidence of the solvent-mediated interconversion between two energetically disparate conformers that feature mutually exclusive interactions. The inherent fluctuations of the water molecules are crucial to the existence of the $n \rightarrow \pi^*$ interactions in the presence of H bonding. The key role of solvent dynamics toward modulating weak interactions, however, could not be previously comprehended from theory and indirect structural data.

These results, though obtained for a small molecule, provide an important and new perspective for the $n \rightarrow \pi^*$ interactions in larger molecular systems. Inherent solvent fluctuation dynamics cause oxygen lone-pair electrons, which are H-bonded to the protic solvents, to intermittently engage in weak $n \rightarrow \pi^*$ interactions. Solute–solvent H-bond formation is expected to be enthalpically favorable over the non-H-bonded conformer. At the same time, this will result in the loss of solvent entropy. Therefore, although the solute has many accessible hydrogen-bonding states, it has been reported that entropy of the total system, which includes the solute and all of the solvent molecules, increases when the solute is not H-bonded.⁴⁸ Thus although enthalpy predicts H bonding, system entropy favors the non-H-bonded species. Moreover, the non-H-bonded PF has an extra enthalpic stabilization arising from the $n \rightarrow \pi^*$ interaction. Thus a concomitant surge in entropic contribution in aqueous solution plausibly maintains the equilibrium between the two energetically unbalanced but competing interactions. The solvent dynamics provides a subtle, yet essential, enthalpy–entropy compensation toward the dynamic equilibrium and helps in the existence of the weak $n \rightarrow \pi^*$ interactions in solution. This is supported by the estimated non-H-bonded population of PF in neat water from MD simulation (see the Supporting Information). Dynamic equilibrium between the H-bonded and non-H-bonded conformers arising from breaking and reformation of C=O H bond is also observed during the MD trajectory.

The picosecond interchange reported in this work hints at critical thermodynamic inferences about $n \rightarrow \pi^*$ interactions from the molecular perspective. Our findings provide the first direct evidence of interconverting H-bonding and weak $n \rightarrow \pi^*$ interactions in aqueous solution. These results demonstrate the potential of similar studies, albeit extremely challenging, to gain a better understanding of $n \rightarrow \pi^*$ interactions in biological and other macromolecular systems in the future.

■ ASSOCIATED CONTENT

Supporting Information

The Supporting Information is available free of charge on the ACS Publications website at DOI: 10.1021/acs.jpcl.8b02398.

Materials, DFT calculations, spectroscopic details, molecular dynamics simulations, Figures S1–S21, and Tables S1–S13 (PDF)

■ AUTHOR INFORMATION

Corresponding Authors

*A.D.: E-mail: a.das@iiserpune.ac.in. Tel: +91-20-25908078.

*S.B.: E-mail: s.bagchi@ncl.res.in. Tel: +91-20-25903048.

*Y.S.K.: E-mail: kimys@unist.ac.kr. Tel: +82-52-217-2530.

ORCID

Aloke Das: 0000-0002-2124-0631

Sayan Bagchi: 0000-0001-6932-3113

Yung Sam Kim: 0000-0001-6306-7438

Author Contributions

#P.D. and G.Y.J. contributed equally to this work.

Notes

The authors declare no competing financial interest.

■ ACKNOWLEDGMENTS

We thank NRF Korea (NRF-2017R1D1A1B03032623 and NRF-2011-0015061), IISER Pune, CSIR-NCL, and SERB India (SR/S2/RJN-142/2012, EMR/2016/000576, and EMR/2015/000486) for funding. P.D. acknowledges DST India for INSPIRE fellowship. We also thank Prof. Kwang S. Kim (UNIST, Korea), Prof. Arnab Mukherjee (IISER Pune, India), and Prof. Anirban Hazra (IISER Pune, India) for helpful discussions.

■ REFERENCES

- (1) Anfinsen, C. B. Principles that Govern the Folding of Protein Chains. *Science* **1973**, *181*, 223–230.
- (2) Dill, K. A. Dominant Forces in Protein Folding. *Biochemistry* **1990**, *29*, 7133–7155.
- (3) Weiss, M. S.; Brandl, M.; Suhnel, J.; Pal, D.; Hilgenfeld, R. More Hydrogen Bonds for the (Structural) Biologist. *Trends Biochem. Sci.* **2001**, *26*, 521–523.
- (4) Nishio, M. The CH/ π Hydrogen Bond in Chemistry. Conformation, Supramolecules, Optical Resolution and Interactions Involving Carbohydrates. *Phys. Chem. Chem. Phys.* **2011**, *13*, 13873–13900.
- (5) Nishio, M.; Umezawa, Y.; Fantini, J.; Weiss, M. S.; Chakrabarti, P. CH– π Hydrogen Bonds in Biological Macromolecules. *Phys. Chem. Chem. Phys.* **2014**, *16*, 12648–12683.
- (6) Dominelli-Whiteley, N.; Brown, J. J.; Muchowska, K. B.; Mati, I. K.; Adam, C.; Hubbard, T. A.; Elmi, A.; Brown, A. J.; Bell, I. A. W.; Cockroft, S. L. Strong Short-Range Cooperativity in Hydrogen-Bond Chains. *Angew. Chem., Int. Ed.* **2017**, *56*, 7658–7662.
- (7) Desiraju, G. R. A Bond by Any Other Name. *Angew. Chem., Int. Ed.* **2011**, *50*, 52–59.
- (8) Arunan, E.; Desiraju, G. R.; Klein, R. A.; Sadlej, J.; Scheiner, S.; Alkorta, I.; Clary, D. C.; Crabtree, R. H.; Dannenberg, J. J.; Hobza, P.; Kjaergaard, H. G.; Legon, A. C.; Mennucci, B.; Nesbitt, D. J. Definition of the Hydrogen Bond (IUPAC Recommendations 2011). *Pure Appl. Chem.* **2011**, *83*, 1637–1641.
- (9) Egli, M.; Gessner, R. V. Stereoelectronic Effects of Deoxyribose O4' on DNA Conformation. *Proc. Natl. Acad. Sci. U. S. A.* **1995**, *92*, 180–184.

- (10) Egli, M.; Sarkhel, S. Lone Pair–Aromatic Interactions: To Stabilize or Not to Stabilize. *Acc. Chem. Res.* **2007**, *40*, 197–205.
- (11) Sarkhel, S.; Rich, A.; Egli, M. Water–Nucleobase “Stacking”: H– π and Lone Pair– π Interactions in the Atomic Resolution Crystal Structure of an RNA Pseudoknot. *J. Am. Chem. Soc.* **2003**, *125*, 8998–8999.
- (12) Hinderaker, M. P.; Raines, R. T. An Electronic Effect on Protein Structure. *Protein Sci.* **2003**, *12*, 1188–1194.
- (13) Bartlett, G. J.; Choudhary, A.; Raines, R. T.; Woolfson, D. N. $n \rightarrow \pi^*$ Interactions in Proteins. *Nat. Chem. Biol.* **2010**, *6*, 615–620.
- (14) Lu, Z.; Gamez, P.; Mutikainen, I.; Turpeinen, U.; Reedijk, J. Supramolecular Assemblies Generated from Both Lone-Pair... π and C–H... π Binding Interactions. *Cryst. Growth Des.* **2007**, *7*, 1669–1671.
- (15) Mooibroek, T. J.; Teat, S. J.; Massera, C.; Gamez, P.; Reedijk, J. Crystallographic and Theoretical Evidence of Acetonitrile– π Interactions with the Electron-Deficient 1,3,5-Triazine Ring. *Cryst. Growth Des.* **2006**, *6*, 1569–1574.
- (16) Choudhary, A.; Kamer, K. J.; Raines, R. T. An $n \rightarrow \pi^*$ Interaction in Aspirin: Implications for Structure and Reactivity. *J. Org. Chem.* **2011**, *76*, 7933–7937.
- (17) Rahim, A.; Saha, P.; Jha, K. K.; Sukumar, N.; Sarma, B. K. Reciprocal Carbonyl–Carbonyl Interactions in Small Molecules and Proteins. *Nat. Commun.* **2017**, *8*, 78.
- (18) Singh, S. K.; Das, A. The $n \rightarrow \pi^*$ Interaction: A Rapidly Emerging Non-Covalent Interaction. *Phys. Chem. Chem. Phys.* **2015**, *17*, 9596–9612.
- (19) Singh, S. K.; Kumar, S.; Das, A. Competition between $n \rightarrow \pi_{Ar}^*$ and Conventional Hydrogen Bonding (N–H...N) Interactions: An Ab Initio Study of the Complexes of 7-Azaindole and Fluorosubstituted Pyridines. *Phys. Chem. Chem. Phys.* **2014**, *16*, 8819–8827.
- (20) Singh, S. K.; Vaishnav, J. K.; Das, A. Experimental Observation of Structures with Subtle Balance between Strong Hydrogen Bond and Weak $n \rightarrow \pi^*$ Interaction: Gas Phase Laser Spectroscopy of 7-Azaindole...Fluorosubstituted Pyridines. *J. Chem. Phys.* **2016**, *145*, 104302.
- (21) Singh, S. K.; Mishra, K. K.; Sharma, N.; Das, A. Direct Spectroscopic Evidence for an $n \rightarrow \pi^*$ Interaction. *Angew. Chem., Int. Ed.* **2016**, *55*, 7801–7805.
- (22) Bartlett, G. J.; Newberry, R. W.; VanVeller, B.; Raines, R. T.; Woolfson, D. N. Interplay of Hydrogen Bonds and $n \rightarrow \pi^*$ Interactions in Proteins. *J. Am. Chem. Soc.* **2013**, *135*, 18682–18688.
- (23) Mooibroek, T. J.; Gamez, P.; Reedijk, J. Lone Pair– π Interactions: A New Supramolecular Bond? *CrystEngComm* **2008**, *10*, 1501–1515.
- (24) Choudhary, A.; Gandla, D.; Krow, G. R.; Raines, R. T. Nature of Amide Carbonyl–Carbonyl Interactions in Proteins. *J. Am. Chem. Soc.* **2009**, *131*, 7244–7246.
- (25) Newberry, R. W.; VanVeller, B.; Guzei, I. A.; Raines, R. T. $n \rightarrow \pi^*$ Interactions of Amides and Thioamides: Implications for Protein Stability. *J. Am. Chem. Soc.* **2013**, *135*, 7843–7846.
- (26) Hamm, P.; Lim, M.; Hochstrasser, R. M. Structure of the Amide I Band of Peptides Measured by Femtosecond Nonlinear-Infrared Spectroscopy. *J. Phys. Chem. B* **1998**, *102*, 6123–6138.
- (27) Park, S.; Kwak, K.; Fayer, M. D. Ultrafast 2D-IR Vibrational Echo Spectroscopy: A Probe of Molecular Dynamics. *Laser Phys. Lett.* **2007**, *4*, 704–718.
- (28) Hochstrasser, R. M. Two-Dimensional Spectroscopy at Infrared and Optical Frequencies. *Proc. Natl. Acad. Sci. U. S. A.* **2007**, *104*, 14190–14196.
- (29) Ghosh, A.; Ostrander, J. S.; Zanni, M. T. Watching Proteins Wiggle: Mapping Structures with Two-Dimensional Infrared Spectroscopy. *Chem. Rev.* **2017**, *117*, 10726–10759.
- (30) Fayer, M. Dynamics of Liquids, Molecules, and Proteins Measured with Ultrafast 2D IR Vibrational Echo Chemical Exchange Spectroscopy. *Annu. Rev. Phys. Chem.* **2009**, *60*, 21–38.
- (31) Kim, Y. S.; Hochstrasser, R. M. Applications of 2D IR Spectroscopy to Peptides, Proteins, and Hydrogen-Bond Dynamics. *J. Phys. Chem. B* **2009**, *113*, 8231–8251.
- (32) Khalil, M.; Demirdöven, N.; Tokmakoff, A. Coherent 2D IR Spectroscopy: Molecular Structure and Dynamics in Solution. *J. Phys. Chem. A* **2003**, *107*, 5258–5279.
- (33) Cho, M. Coherent Two-Dimensional Optical Spectroscopy. *Chem. Rev.* **2008**, *108*, 1331–1418.
- (34) Hamm, P.; Zanni, M. *Concepts and Methods of 2R Infrared Spectroscopy*; Cambridge University Press: Cambridge, U.K., 2011.
- (35) Foster, J. P.; Weinhold, F. Natural Hybrid Orbitals. *J. Am. Chem. Soc.* **1980**, *102*, 7211–7218.
- (36) Edington, S. C.; Flanagan, J. C.; Baiz, C. R. An Empirical IR Frequency Map for Ester C=O Stretching Vibrations. *J. Phys. Chem. A* **2016**, *120*, 3888–3896.
- (37) Chuntunov, L.; Pazos, I. M.; Ma, J.; Gai, F. Kinetics of Exchange between Zero-, One-, and Two-Hydrogen-Bonded States of Methyl and Ethyl Acetate in Methanol. *J. Phys. Chem. B* **2015**, *119*, 4512–4520.
- (38) Pazos, I. M.; Ghosh, A.; Tucker, M. J.; Gai, F. Ester Carbonyl Vibration as a Sensitive Probe of Protein Local Electric Field. *Angew. Chem., Int. Ed.* **2014**, *53*, 6080–6084.
- (39) Kashid, S. M.; Bagchi, S. Experimental Determination of the Electrostatic Nature of Carbonyl Hydrogen-Bonding Interactions Using IR-NMR Correlations. *J. Phys. Chem. Lett.* **2014**, *5*, 3211–3215.
- (40) Kashid, S. M.; Jin, G. Y.; Chakrabarty, S.; Kim, Y. S.; Bagchi, S. Two-Dimensional Infrared Spectroscopy Reveals Cosolvent-Composition-Dependent Crossover in Intermolecular Hydrogen-Bond Dynamics. *J. Phys. Chem. Lett.* **2017**, *8*, 1604–1609.
- (41) Bagchi, S.; Charnley, A. K.; Smith, A. B.; Hochstrasser, R. M. Equilibrium Exchange Processes of the Aqueous Tryptophan Dipeptide. *J. Phys. Chem. B* **2009**, *113*, 8412–8417.
- (42) Kashid, S. M.; Jin, G. Y.; Bagchi, S.; Kim, Y. S. Cosolvent Effects on Solute–Solvent Hydrogen-Bond Dynamics: Ultrafast 2D IR Investigations. *J. Phys. Chem. B* **2015**, *119*, 15334–15343.
- (43) Kim, Y. S.; Hochstrasser, R. M. Chemical Exchange 2D IR of Hydrogen-Bond Making and Breaking. *Proc. Natl. Acad. Sci. U. S. A.* **2005**, *102*, 11185–11190.
- (44) Zheng, J.; Kwak, K.; Asbury, J.; Chen, X.; Piletic, I. R.; Fayer, M. D. Ultrafast Dynamics of Solute–Solvent Complexation Observed at Thermal Equilibrium in Real Time. *Science* **2005**, *309*, 1338–1343.
- (45) Kim, Y. S.; Hochstrasser, R. M. Comparison of Linear and 2D IR Spectra in the Presence of Fast Exchange. *J. Phys. Chem. B* **2006**, *110*, 8531–8534.
- (46) Woutersen, S.; Mu, Y.; Stock, G.; Hamm, P. Hydrogen-Bond Lifetime Measured by Time-Resolved 2D-IR Spectroscopy: N-Methylacetamide in Methanol. *Chem. Phys.* **2001**, *266*, 137–147.
- (47) Newberry, R. W.; Orke, S. J.; Raines, R. T. $n \rightarrow \pi^*$ Interactions Are Competitive with Hydrogen Bonds. *Org. Lett.* **2016**, *18*, 3614–3617.
- (48) Mukherjee, A. Entropy Balance in the Intercalation Process of an Anti-Cancer Drug Daunomycin. *J. Phys. Chem. Lett.* **2011**, *2*, 3021–3026.